Earth and Planetary Science Letters 422 (2015) 87–93

Contents lists available at ScienceDirect

Earth and Planetary Science Letters

www.elsevier.com/locate/epsl

Three-dimensional electrical resistivity of the north-central USA from EarthScope long period magnetotelluric data

Bo Yang [a,b,*], Gary D. Egbert [b,**], Anna Kelbert [b], Naser M. Meqbel [c]

[a] Hubei Subsurface Multi-scale Imaging Key Laboratory, Institute of Geophysics and Geomatics, China University of Geosciences, Wuhan, China
[b] College of Earth, Ocean, and Atmospheric Sciences, Oregon State University, Corvallis, OR, USA
[c] Research Centre for Geosciences-Potsdam (GFZ), Potsdam, Germany

ARTICLE INFO

Article history:
Received 30 December 2014
Received in revised form 2 April 2015
Accepted 6 April 2015
Available online 23 April 2015
Editor: P. Shearer

Keywords:
EarthScope
USArray
Midcontinent rift
MT
suture zone

ABSTRACT

We present initial results from three-dimensional inversion of long period EarthScope magnetotelluric (MT) transportable array data from 232 sites covering the north-central US. The study area covers the 1.1 Ga Mid-Continent Rift (MCR) system, which cuts across a series of Archean and Paleoproterozoic lithospheric blocks. The western arm of the MCR is clearly evident in shallow depth sections, with a narrow resistive core, flanked by elongate conductive basins. Other prominent upper-crustal features mapped include the moderately conductive Michigan and Illinois Basins, and extremely high conductivities in foreland basin rocks at the southern margin of the Superior craton. The most prominent conductive anomalies, in an otherwise relatively resistive mid-lower crust, are two elongate east–west oriented structures, which are closely aligned with previously inferred continental sutures. The first underlies the southern margin of the Superior craton just north of the Niagara Fault (NF), and can be associated with the ~1.85 Ga Penokean Orogeny. A second, further south beneath Iowa and western Wisconsin, lies just south of the Spirit Lake tectonic zone (SLtz), and can be identified with Yavapai accretion at ~1.75 Ga. Both of these conductive sutures are cleanly cut by the MCR, which is otherwise not clearly evident in the deeper parts of the resistivity model. The break in the anomalies is narrow, comparable to the surface expression of the MCR, indicating that rifting impacts on the entire crustal section were highly localized. Both suture-related anomalies are imaged as extending into, and perhaps through, the lithosphere as dipping diffuse zones of reduced mantle resistivity. Sense of dip of these structures (southward for the NF anomaly, northward for SLtz) agrees with previously inferred models for subduction and accretion, suggesting that a conductive phase (most likely carbon) has been thrust deep into the lower crust and uppermost mantle, providing a marker of the three-dimensional boundary between lithospheric blocks. Resistivities drop below ~100 Ω m below ~200 km depth, in rough agreement with the seismically determined lithosphere–asthenosphere boundary (LAB). There are modest lateral variations in this deep low-resistivity layer, but the reliability and significance of these are not yet clear.

1. Introduction

The magnetotelluric (MT) component of the EarthScope USArray program is a powerful tool for regional-scale imaging of deep 3D electrical resistivity variations in the North American crust and upper mantle (e.g., Meqbel et al., 2014). Here we present results from the second EarthScope long period MT data footprint, consisting of 232 sites covering the north-central USA, collected during 2011–2013 with the seismic transportable array nominal site spacing of 70 km. In contrast to the tectonically active Northwestern United States covered by the first footprint (Patro and Egbert, 2008; Zhdanov et al., 2011; Meqbel et al., 2014; Bedrosian and Feucht, 2014), this area has been stable over at least the entire Phanerozoic. The most recent significant geotectonic event, at 1.1 Ga, was the development of the mid-continent rift (MCR), by far the most notable geophysical anomaly in the region, especially in gravity and magnetics (e.g., Hildebrand, 1985; Chandler et al., 1989). The MCR cuts across geological provinces of much greater age (e.g., Hoffman, 1989), from the Archean Superior Province in the north to the Paleoproterozoic Yavapai and Mazatzal Provinces in the south (Fig. 1).

* Principal corresponding author.
** Corresponding author.
E-mail addresses: yangbo@cug.edu.cn (B. Yang), egbert@coas.oregonstate.edu (G.D. Egbert).

http://dx.doi.org/10.1016/j.epsl.2015.04.006
0012-821X/

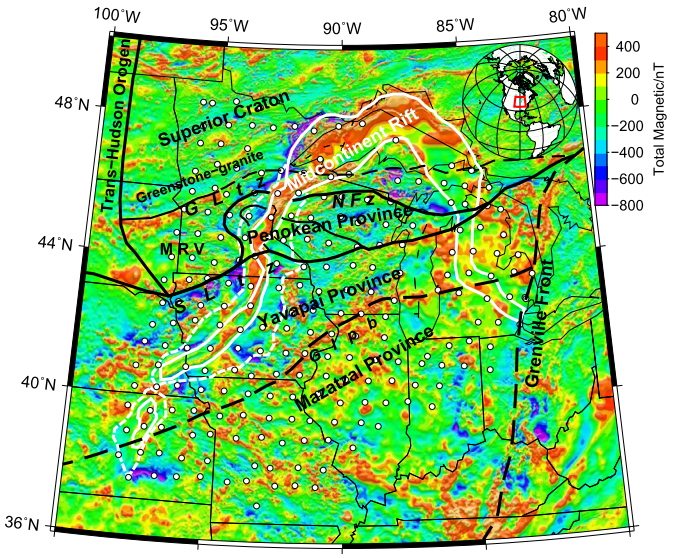

Fig. 1. Map of study area, showing magnetic anomaly map (USGS website: http://mrdata.usgs.gov/magnetic/); MT site locations (white circle), geologic terrane map of Precambrian basement rocks (after Holm et al., 2007 and Renee Rohs and Van Schmus, 2007); MCR boundaries (after Renee Rohs and Van Schmus, 2007); GIpb: Green Island plutonic belt; GLtz: Great Lakes tectonic zone; MRV: Minnesota River Valley subprovince; NFz: Niagara Fault zone; SLtz: Spirit Lake tectonic zone.

Modern interpretations of the study area, based primarily on precise geochronology and refined compilations of potential field data, are summarized in Holm et al. (2007), with further details and graphical summaries of accretionary events provided by Van Schmus et al. (2007) (Fig. 6) and Schulz and Cannon (2007) (Fig. 6). In this area, the Superior Province is divided into the Greenstone–Granite (2.6–3.6 Ga), and the Minnesota River Valley (3.4–3.6 Ga) subprovinces, respectively south and north of the Great Lakes tectonic zone (GLtz; Fig. 1). South of the Superior Province and east of Minnesota River Valley lies the Penokean Province, accreted between 1.8 and 1.9 Ga. On the surface, the boundary between the Superior and Penokean Provinces is defined by the Niagara Fault zone (NF). To the north, extensive foreland basin rocks lap onto the craton margin domain, an assemblage consisting of sedimentary and volcanic rocks deposited during the interval 2.3–1.77 Ga (Holm et al., 2007). The Penokean Province, and the Minnesota River Valley to the west, are bounded on the south by the Spirit Lake tectonic zone (SLtz; Fig. 1), marking the transition to the Yavapai Province, accreted at 1.7–1.8 Ga. First identified in the more exposed southwest USA, the juvenile arc rocks of the Yavapai Province are now generally thought to extend into southern Ontario (Van Schmus et al., 2007). Assembly of the continent in this area was completed with accretion of the Mazatzal province at 1.6–1.7 Ga.

The final important regional tectonic event was creation of the MCR at 1.1 Ga. In the standard interpretation (e.g., Keller et al., 1983), the MCR represents a failed continental rift. Geochemistry of exposed rift basalts, mostly near Lake Superior, suggests that a mantle plume may have initiated rifting (Nicholson et al., 1997). The rifting was terminated within ~30–50 m.y., possibly due to a change in the compressional stress regime associated with initiation of the Grenville Orogeny (e.g., Cannon and Hinze, 1992), as indicated by thrust faulting on the flanks (Cannon, 1994), and thickened crust underlying the rift (Shen et al., 2013). Stein et al. (2014) offered an alternative interpretation of MCR evolution, suggesting that the rifting was initiated as part of successful larger-scale continental rifting of Amazonia from Laurentia, which became inactive in the interior once seafloor spreading was established.

Although the MCR was a major target of the second EarthScope MT footprint, we will show that the most striking conductivity anomalies in this region, which generally has moderately resistive lithosphere, are associated with two Paleoproterozoic suture zones resulting from Penokean and Yavapai subduction and accretion. At least the near surface expressions of some of these conductive features have been glimpsed by previous EM studies (Sternberg and Clay, 1977; Boerner et al., 1996), but here we provide a more comprehensive 3D regional view, extending to asthenospheric depths. Except in the upper crust, resistivity variations associated with the MCR are more subtle. Indeed, the deep structure of the MCR is most clearly expressed in our resistivity images as gaps cut through the evidently older lower crustal conductive structures.

2. Magnetotelluric data and inversion

The EarthScope MT data were acquired using long period instruments based on fluxgate magnetometers, and were processed using a standard robust remote reference algorithm (Egbert and Booker, 1986; Egbert, 1997) to produce impedances (**Z**) and vertical transfer functions (VTFs). The data quality is very good for most stations, although a few sites near densely populated area were contaminated by cultural noise, and were omitted for the inversions shown here.

We employed the Modular system for Electromagnetic Inversion (ModEM, Egbert and Kelbert, 2012; Kelbert et al., 2014) for 3D modeling and inversion. The 3D resistivity model presented in this study was obtained by jointly inverting the full impedance and VTFs from 222 stations (Fig. 1) at 28 periods, ranging from 11 s to 18 725 s for **Z**. For VTFs, only periods shorter than 7281 s were used to avoid biases due to finite source spatial scale, a more serious problem for VTFs than for impedances (e.g., Dmitriev and Berdichevsky, 1979). The data are presented and discussed further in the Supplementary material.

We assigned error floors of 5% of $|Z_{xy} \cdot Z_{yx}|^{1/2}$ for all four **Z** components and a constant value of 0.03 for VTFs, comparable to levels used in previous regional scale 3D inversions (e.g. Meqbel et al., 2014; Bedrosian and Feucht, 2014). The study area was discretized with a 20 km grid in the core, padded with 7 cells on all edges, with widths increasing by a factor of 1.2 outward to the boundary. Vertically, 54 layers were used, starting from 50 meters and increasing logarithmically with a factor of 1.12. This discretization resulted in a $98 \times 83 \times 61$ grid, in the x, y and z directions, including 7 air layers. Note that the Great Lakes are relatively shallow (roughly 100 m on average) with resistivity close to 100 Ω m (Doherty, 1963), so we have not deemed it necessary to include lake bathymetry in prior models.

Eighteen runs have been conducted varying inversion parameters, (e.g., length scales of model smoothing), subsets of data fit (impedances only, impedance and VTFs jointly, subsets of periods), and prior models (100 Ω m half-space, 200 Ω m half-space, 1D layered model). As in Meqbel et al. (2014), we rely on a fine enough parameterization of the uppermost layers to accommodate near surface distortion. To further reduce possible near surface static shift effects, for some inversion runs we tested a strategy of reducing the smoothing parameters for layers shallower than 2 km. This produced rougher shallow structure, and concentrated high and low resistivities in the near surface layers, resulting in slightly smoother and simpler deep structure. We used this strategy for the preferred inverse solution shown below. For this solution, we first fit **Z** only, adopting a 100 Ω m half-space prior model. Convergence, to a normalized root mean square misfit (nRMS) of 1.83, required 130 iterations of the nonlinear conjugate gradient (NLCG) scheme used in ModEM. We then restarted the inversion to fit **Z** and VTFs jointly, using an additional 112 iterations to fit the full dataset to a nRMS of 1.84. Adding the VTF data resulted in some-

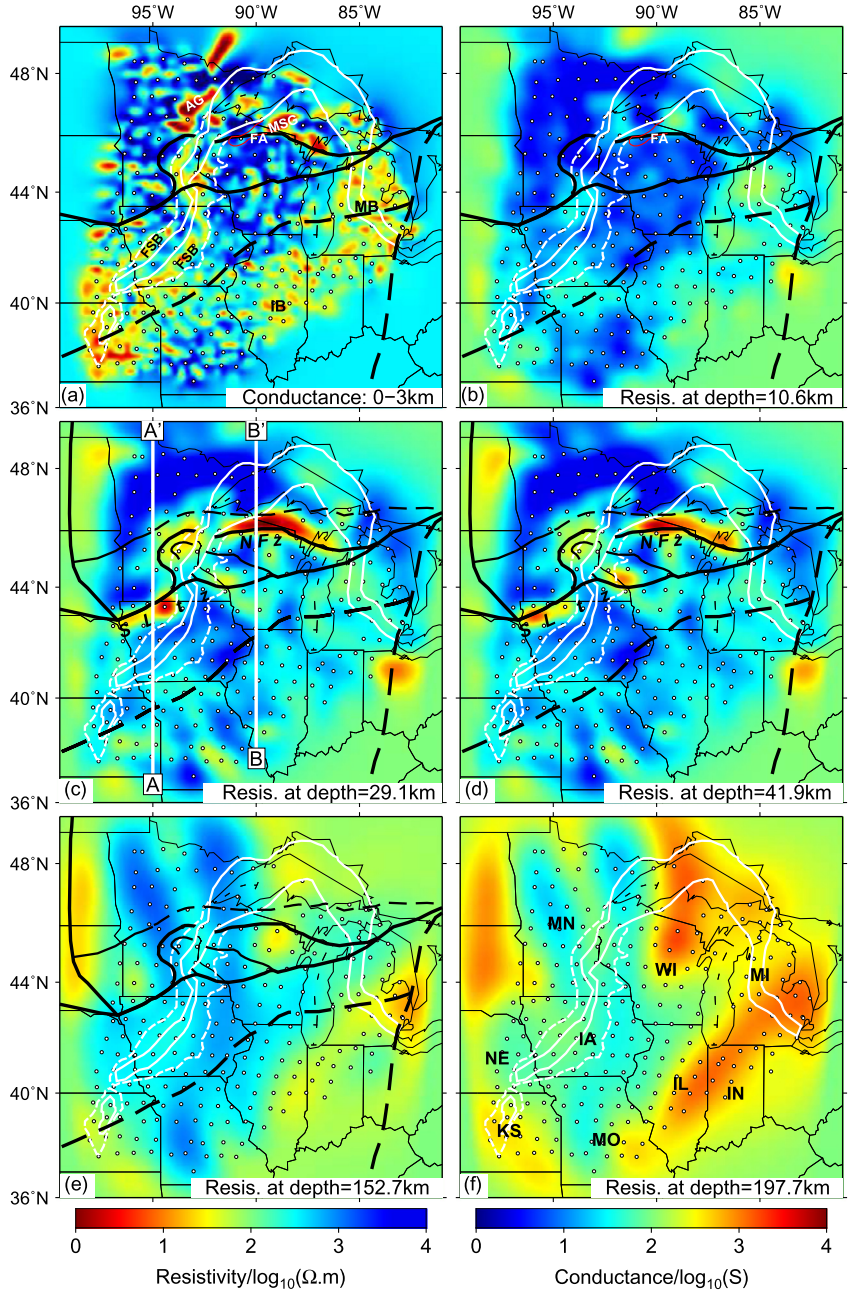

Fig. 2. Resistivity inverse model. (a) Conductance (vertically integrated conductivity) for depth range of 0–3 km. (b)–(d) electrical resistivity at representative crustal and upper mantle depths. MCR is indicated by white lines, and MT site locations are marked by white circles. Tectonic zones and terrane boundaries are indicated by black outlines following Fig. 1. South–North white profiles A–A′ and B–B′ in (c) give locations of vertical cross-sections shown in Fig. 3. AG: Animikie Group; FA: Flambeau Anomaly; FSB: Flanking Sedimentary Basin; IB: Illinois Basin; MB: Michigan Basin; MSG: Marquette Supergroup. IA: Iowa; IL: Illinois; IN: Indiana; KS: Kansas; MI: Michigan; MN: Minnesota; MO: Missouri; NE: Nebraska; WI: Wisconsin.

what clearer and more continuous images of conductivity anomalies, as shown in the Supplementary material.

3. Results and discussion

The recovered 3D electrical resistivity model, which we present in selected depth slices and cross-sections, shows regional structure from crust to upper mantle. A nominal skin depth in 100 Ω m background is already 15 km at the shortest periods, suggesting limited vertical resolution at shallow depths. Sensitivity tests for principal model features are discussed in the Supplementary material.

3.1. Shallow structure

To display the near-surface model heterogeneity, we plot the surface electrical conductance, defined as the conductivity integrated over all layers shallower than 3 km in Fig. 2(a). In reality, some of the conductance we have mapped to the upper 3 km may be distributed over an even thicker upper crustal section. Furthermore, the shallow conductance map is somewhat “spotty” with isolated conductive and resistive features at the site spacing scale. This appearance results from use of a regularization approach which penalizes differences from a prior model (which the inverse solution reverts to if possible), and reflects the weak sensitivity of the MT data to near surface resistivity between the

widely spaced sites. Static distortion, and our strategy of reducing model smoothing in the upper layers to better fit these near surface effects, exacerbates this problem. In spite of these effects and associated uncertainties, the shallow conductance map shows strong consistency with known surface geological features. For example, the Michigan Basin, which has subsided for 500 m.y., with about 4 km of Phanerozoic sediments accumulated at its center (Sleep and Sloss, 1978), and the Illinois Basin, filled during the Paleozoic with up to 6 km of sediments (Heidlauf et al., 1986), are both clearly delineated.

Narrow conductive sedimentary basins flank the resistive plutonic core of the MCR, most clearly in Iowa and southern Minnesota, consistent with gravity and magnetics (Hinze et al., 1992), and seismic imaging (Shen et al., 2013). Segmentation of the rift, evident in the "pinch out" of the gravity high in southern Minnesota is also clearly present in the surface conductance map (Fig. 2(a)). The expression of the MCR in the surface resistivity images is less clear beneath Lake Superior (where there is no MT data) and on the eastern arm (where the rift is buried beneath the conductive sediments of the Michigan Basin). High surface conductivities are also seen in eastern Kansas and Nebraska, consistent with thick sedimentary cover in this area (e.g., Newell and Hatch, 2000). Interestingly, there is a narrow north-south trending resistive patch just east of a similarly shaped gravity high outlined in Fig. 2(a), which is generally inferred to be the buried southernmost section of the MCR. The resistivity images suggest that (at least near the surface) the core of the MCR may lie further to the east.

The most prominent features in the surface conductance map of Fig. 2(a) lie north of the NF, on either side of the MCR. These patches, which have conductance of 1000 S or more, correspond approximately to surface exposures of the Animikie Group and Marquette Supergroup, synorogenic foredeep sedimentary sequences, including euxinic shales and turbidites. These overly passive margin sediments, and abut the heavily deformed fold and thrust belts along the north edge of the NF.

Low resistivities in the vicinity of the NF have been detected by two previous EM surveys. Sternberg and Clay (1977) reported results from very long dipole DC soundings, including long-range high-power transmissions obtained during tests of US Navy communication antennas at Clam Lake, Wisconsin. These soundings detected a very conductive anomaly (referred to as the Flambeau anomaly) covering the area outlined in Fig. 2(a). Based on 2D forward modeling tests, it was inferred that the anomaly extended to depths of ∼10 km, with a conductance exceeding 1000 S. Sternberg and Clay (1977) also summarize results from an industry airborne EM survey conducted in this area, which mapped a series of narrow (∼1 km wide) elongate near-surface conductive features in the area. These were subsequently drilled, recovering sections with high concentrations of graphite and pyrite, with bulk resistivities as low as 0.03 Ω m. A second early MT survey (Wunderman, 1988), summarized in Boerner et al. (1996), mapped a highly conductive zone west of the MCR, near the Animikie Group conductive feature in our model, in an area of outcropping graphitic schists (Southwick and Morey, 1990).

As mapped by Sternberg and Clay (1977), the Flambeau anomaly is relatively localized, and does not explicitly coincide with any of the conductive surficial patches in our models. Similarly, the results from Wunderman (1988) are only qualitatively consistent with our maps of surface features. This suggests that caution should be used in interpreting fine scale details of our resistivity maps (based on a very coarse 70 km site spacing), particularly at shallow depths. However, we consider it likely that the conductive zones mapped in detail by these previous high resolution local surveys bear a close genetic relationship to the broader-scale patterns revealed by the MT transportable array.

The mid-crust (Fig. 2(b)) is generally resistive north of the Yavapai–Mazatzal Province boundary, in the Superior Province exceeding 3000 Ω m on average. Typical resistivities in the Yavapai Province and Mazatzal Province are lower at this depth, 300–1000 Ω m. Patches of lower resistivity (∼100 Ω m) are seen locally, particularly beneath the very conductive surface features north of the NF, and the conductive basins. Given the limited vertical resolution of our band-limited data, vertical extents of conductive surficial features in Fig. 2(a) are poorly constrained. For example, while all inverse solutions clearly show increasing resistivity in the mid-crust, depth to bottom for the very conductive features along the southern edge of Superior Province varied between inversion runs, depending on smoothing parameters assumed.

3.2. Conductive sutures

The two middle panels in Fig. 2(c, d) show resistivities in the lower-crust extending to near the Moho, which is at ∼45–50 km (Keller, 2013). The most striking features in these depth sections are two elongate E–W conductive zones, which coincide almost perfectly with the Penokean and Yavapai Province terrane boundaries mapped on the surface, i.e., the NF and SLtz. We thus henceforth refer to these two lower crustal conductive zones as the NF and SLtz anomalies, respectively. The NF (northern) anomaly extends across, but is broken by, the MCR. The eastern segment is continuous over 400 km, tracking the NF fault just to the south almost perfectly. The more diffuse and less conductive section to the west is also well aligned with the complex bending surface expression of the NF in Minnesota. Sections to the east and west of the MCR underlie, and may be associated with, the Marquette Supergroup and Animikie Group surficial conductors, respectively, but the model implies that there need be no direct conductive connection.

A second conductive anomaly lies just south of the SLtz in Iowa, continuing more weakly to the east of the MCR in western Wisconsin, here just north of the SLtz. Basement exposure is very limited in the vicinity of the SLtz anomaly, and the top of the conductor is in this case clearly at mid-lower crustal depths. The SLtz has minimal shallow expression in resistivity, with only two small high conductance spots evident in the near surface layer. While the SLtz conductive anomaly has not been previously mapped, a deep conductive suture related to Yavapai accretion was identified in the Cheyenne Belt in southern Wyoming by Meqbel et al. (2014, see also Boerner et al. 1996, and references therein).

Both conductive anomalies extend across, but are cleanly broken by, the MCR. The anomalies extend nearly to the edges, implying that the MCR is a high-angle structure through the entire crust. This result is consistent with crustal density beneath the west arm of the MCR inferred from modeling gravity data (Merino et al., 2013), but is more definitive.

Vertical sections (Fig. 3) show that while the two anomalies are concentrated in the crust, they continue more weakly into the mantle, possibly extending through the lithosphere. The NF anomaly is associated with a broad zone of moderately low resistivity (200–500 Ω m; section B–B′) dipping to the south, consistent with the inferred sense of subduction associated with the Penokean orogeny (e.g., Van Schmus et al., 2007). The SLtz also extends into the mantle, with a clear north-dipping zone of low resistivity (100–200 Ω m; section A–A′), cutting through the lithosphere. Sense of dip is again consistent with tectonic models for Yavapai accretion (Van Schmus et al., 2007).

Low resistivities have been frequently observed along terrane boundaries and sutures, and are most often explained by graphite and/or sulfides metamorphosed and emplaced within the crust

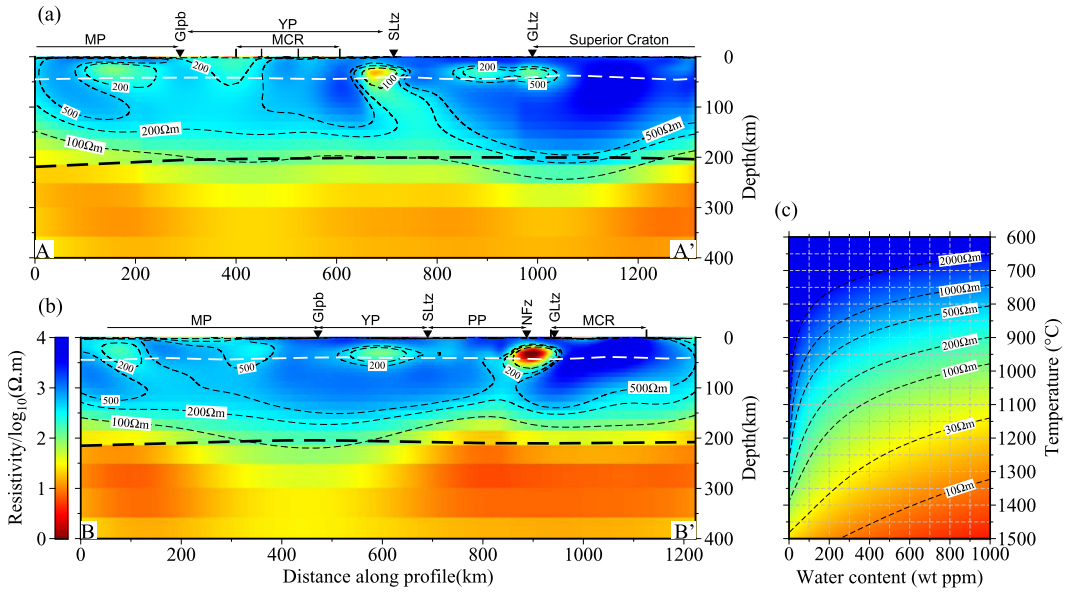

Fig. 3. Representative cross sections (lines A–A′ and B–B′ in Fig. 2(c)). The white dashed line indicates the Moho location from the CRUST 1.0 model (http://igppweb.ucsd.edu/~gabi/rem.html). The black dashed line indicates the LAB from the seismic model of Yuan et al. (2014). MCR: Midcontinent Rift; MP: Mazatzal Province; PP: Penokean Province; YP: Yavapai Province. Panel (c) shows olivine resistivity computed from laboratory results of Dai and Karato (2014) as a function of temperature and water content, using same color scale. Resistivity for dry olivine is from SEO3 (Constable, 2006).

during subduction and orogenesis (e.g., Boerner et al., 1996; Jones et al., 2005; Wannamaker, 2005). Boerner et al. (1996) pointed out that many conductive anomalies mapped in North America could be associated with euxinic carbonaceous shales, initially deposited in Paleoproterozoic foredeeps, and subsequently graphitized and concentrated in fold and thrust belts by subduction related deformation. Conductive suture zones are also found in other (non-foredeep) environments, such the broad continent/continent collision zone of the Trans-Hudson Orogen, marked by the continental scale North American Central Plains Conductivity Anomaly (NACPCA; Camfield and Gough, 1977). Jones et al. (2005) review a number of MT studies of the NACPCA, showing that narrow semi-continuous zones of macro-anisotropic (connected along strike, but not across) low resistivity occur all along the suture zone. The anomalies can often be associated in outcrop with sheared graphitic metasediments and sulfide mineralization, again implicating interconnected sheets of these highly conducting phases in the observed conductive anomalies. We suggest a similar explanation here, although some questions are raised by the depth of the anomalies. Laboratory measurements of Yoshino and Noritake (2011) with carbon films on quartz suggest that due to surface tension, thin graphitic films on grain boundaries might not remain interconnected in the lower crust on geologic time scales. However, thicker layers or veins of graphite would not suffer from this problem, and sulfides could conceivably be concentrated and remain interconnected at lower crustal conditions (Ducea and Park, 2000).

Much of the evidence for conductive sutures (e.g., as discussed in Boerner et al., 1996 and Jones et al., 2005) has been provided by high-frequency MT surveys, and thus relatively shallow (mid-upper crustal) conductive anomalies have most often been emphasized. For example, only recently have possible deep extensions of the NACPCA into the mantle been noted (Jones et al., 2005). Our long-period MT results emphasize further that material deposited at a convergent margin may be carried to great depth during subduction and orogenesis, to create coherent conductive anomalies extending through the lower crust and into the mantle. Conductivities of the two sutures imaged here peak in the lower crust, but appear to continue through the entire mantle lithosphere as diffuse dipping zones of modest resistivity (100–200 Ω m). In interpreting these features it is important to bear in mind that only the conductance of this dipping structure is constrained. A thinner layer of much lower resistivity (e.g., a zone of 10 km width, and 10 Ω m resistivity) would be indistinguishable from the roughly 100 km thick 100 Ω m layer in the inverse solution.

Given the great age of the suture zones, free fluids, which would be gravitationally unstable, cannot plausibly explain the low resistivities of mantle (or crustal) anomalies. For a reasonable cratonic geotherm (e.g., McKenzie et al., 2005; Hasterok and Chapman, 2011) temperatures from the Moho to ∼150 km depth would be too low (i.e., 600–1000 °C) to explain observed resistivities with plausible hydration levels, even with the most optimistic laboratory based models for olivine conductivity (Dai and Karato, 2014). It is possible that these models are still leaving out important conduction mechanisms, as suggested by Jones et al. (2012). Another possible explanation is that the dipping conductive layers also contain interconnected graphitic carbon (or sulfides), possibly in a relatively thin layer marking the accretionary boundary between the subducted and overriding blocks, as suggested for the Slave craton by Jones et al. (2003). Similar conductivity enhancement by carbon has been inferred for the uppermost mantle lithosphere along the southern edge of the Hearne craton by Nieuwenhuis et al. (2014). Experimental results of Wang et al. (2013) suggest that ∼1% graphite could reduce olivine resistivity to ∼10 Ω m at lithospheric temperatures, assuming sufficiently reducing conditions. Near the bottom of the lithosphere, below the graphite/diamond stability field (∼140 km) this explanation obviously could not hold, but temperatures at these depths would be high enough to match observed resistivities with only modest levels of hydration (∼100 wt ppm; see Fig. 3). In this scenario the fossil subduction zones would contain both higher levels of hydration, and other conductive phases, which together would contribute to enhancing conductivity over the full depth range.

While the clear geometric association between the dipping low resistivity layers in the lithosphere and previously mapped terrane boundaries suggests a causal link to ancient subduction, it should be noted that there are other parts of the mantle lithosphere, particularly within the accreted Paleoproterozoic terranes to the south, with comparably low resistivities. It is worth noting that similarly low resistivities (∼200–300 Ω m) have been observed in

the lithosphere to the southeast, beneath the Appalachian Plateau (Ogawa et al., 1996; Wannamaker, 2005). At least at shallow depths these areas also appear to be too conductive to be explained by current models of hydrated olivine. Arguably this is further evidence for additional, as yet poorly understand, conduction mechanisms, and the need for caution in interpretation of laboratory results (Jones et al., 2012). It may also reflect widespread presence of conductive phases such as graphite in these juvenile arc terranes.

3.3. Asthenosphere

A clear transition to lower resistivities occurs near 200 km depth (Fig. 3), broadly consistent with estimates from seismology of depth to the lithosphere–asthenosphere boundary (LAB) in this area (Yuan and Romanowicz, 2010; Yuan et al., 2014). For an asthenospheric potential temperature of 1300 °C, resistivity (at ~200 km depth) of dry olivine inferred from models based on laboratory measurements (SEO3, Constable, 2006) is roughly 100 Ω m. As a reference we plot this contour on the cross-sections of Fig. 3. Since mantle conductivity could be enhanced by hydrogen (or other conductive phases) this represents a minimum depth to the LAB. Although broadly consistent with the seismic LAB, the resistivity contour exhibits much greater lateral depth variation. This difference may reflect the relatively low resolution (1×1 degree) of the seismic model, or artifacts in the resistivity model–perhaps due to biases introduced by near surface distortion, or vertical smearing from lateral variations in more deeply seated (asthenospheric) low resistivities. It is also at least possible that variations in depth of the 100 Ω m contour reflect lateral variations in deep lithospheric hydration. Rather speculatively, the broad N–S zone of relatively reduced resistivities in the center of the array (Fig. 2f) may represent more depleted lithosphere that has been influenced by melting associated with the MCR. Further tests with the MT data, combined with higher resolution regional seismic investigations are warranted to explore these issues more fully.

Deep resistivities (below 200 km) are also laterally variable, ranging between 10 and 30 Ω m. These high conductive values are not consistent with laboratory models for dry olivine; e.g., the SEO3 model would require temperatures of 1500–1600 °C. However, using the model of Dai and Karato (2014) these resistivities can be readily explained with fairly modest levels of hydration (~200–400 wt ppm H_2O). Again, these variations in deep resistivity warrant more thorough testing.

4. Conclusions

The most striking, and clearly resolved (see Supplementary material), structures imaged by the EarthScope "MCR" footprint, are two elongate lower crustal conductive anomalies. Both the SLtz and NF anomalies are clearly associated with relict sutures that record Paleoproterozoic accretionary events. The MCR is expressed most clearly in the deep resistivity images through gaps introduced into these conductive structures by the rifting event. The sharp (nearly vertical) gaps indicate that here rifting was very high-angle, with minimal impact on pre-existing lithospheric structure. This demonstrates clearly how conductive anomalies introduced during ancient tectonic processes can serve as stable long-lived markers that can be imaged in three dimensions to provide valuable constraints on ancient and deep structures and processes.

While many conductive suture zones have been previously identified from 2D MT profile data, widely spaced but spatially extensive array data of the sort considered here offers new opportunities for mapping and understanding the often cryptic process of continental assembly. In particular, the 3D imaging made possible by these data allows constraints on along strike variations (such as the gaps associated with the MCR), and (at least at a broad scale) linking in three dimensions structures that may extend from the surface into the mantle. An important result of this study is that in some suture zones conductive structures extend from near surface, to the lower crust, and through the mantle lithosphere. This suggests that conductive phases (graphite and sulfides) can be carried deep into the Earth during subduction and orogenesis. The large area covered by an array is also quite useful for reconnaissance, revealing unknown structures, such as the SLtz anomaly, and providing broad scale 3D information, such as the dip of a contact or suture, that may be cryptic or ambiguous from surface geology.

Of course, the large scale of the transportable array MT data considered here leaves many details unresolved. For example, the imaged suture zones are almost certainly anisotropic, reflecting substantial fine scale layering and structure in the conductive rocks in the core of the anomaly. Furthermore, important details about the relationship between surficial features and deeper anomalies are poorly resolved by the wide site spacing and limited bandwidth. Higher resolution broad band MT studies of specific areas will be essential to fill in such important details.

Contrasts between the resistivities of the two areas in North America now covered by EarthScope MT array data are worth noting. Aside from the conductive suture zones, variations of resistivity from the middle crust into the uppermost mantle are relatively subdued in the north-central US. In particular, here in the stable continental interior there is no evidence for sub-horizontal conductive layers near the Moho, which are ubiquitous in the tectonically active parts of the northwestern US (Meqbel et al., 2014). Although this result is not surprising, given that this cratonic area has been quiescent over the entire Phanerozoic, it does offer further support for the now standard interpretation (e.g., Wannamaker et al., 1997) of these extensive lower crustal conductive layers as transient features composed of fluids and melt associated with active tectonic and magmatic processes. There are also significant differences in mantle resistivity in the two areas. Although we have noted some variations in the deep resistivity in the north-central US, the deep structure is actually comparatively uniform. Variations in depth to reduced (nominally asthenospheric, ~100 Ω m) resistivities are much greater in the west. Again, this is not unexpected, as lithospheric thickness is relatively constant across the north-central US, but varies widely in the west, in a manner quite consistent with the deep resistivity variations imaged by Meqbel et al. (2014). Taken together, results from the two EarthScope footprints clearly demonstrate that the LAB does have a reasonably consistent electrical signature, which can be mapped with a widely spaced array of long period MT sites. However, as our rather preliminary results above suggest there is still much to understand about deep conductivity of the lithosphere and asthenosphere, and relationships with seismic constraints. Integration of these two geophysical datasets could offer new insights into the nature of the LAB.

Acknowledgements

This research was supported by National Natural Science Foundation of China (NSFC) grants 41304110 and 41374079, NSF grant EAR1053628 and partly by the Special Fund for Basic Scientific Research of Central Colleges, China University of Geosciences, Wuhan (#CUG090106 and #CUGL100402). We thank the two anonymous reviewers for their comments and suggestions.

Appendix A. Supplementary material

Supplementary material related to this article can be found online at http://dx.doi.org/10.1016/j.epsl.2015.04.006. These data include the Google map of the most important areas described in this article.

References

Bedrosian, P.A., Feucht, D.W., 2014. Structure and tectonics of the northwestern United States from EarthScope USArray magnetotelluric data. Earth Planet. Sci. Lett. 402, 275–289. http://dx.doi.org/10.1016/j.epsl.2013.07.035.

Boerner, D.E., Kurtz, R.D., Craven, J.A., 1996. Electrical conductivity and Paleo-Proterozoic foredeeps. J. Geophys. Res., Solid Earth 101 (B6), 13775–13791. http://dx.doi.org/10.1029/96JB00171.

Camfield, P.A., Gough, D.I., 1977. A possible Proterozoic plate boundary in North America. Can. J. Earth Sci. 14 (6), 1229–1238. http://dx.doi.org/10.1139/e77-112.

Cannon, W.F., 1994. Closing of the Midcontinent rift — a far-field effect of Grenvillian compression. Geology 22 (2), 155–158. http://dx.doi.org/10.1130/0091-7613(1994)022<0155:COTMRA>2.3.CO;2.

Cannon, W.F., Hinze, W.J., 1992. Speculations on the origin of the North American Midcontinent rift. Tectonophysics 213, 49–55.

Chandler, V.W., McSwiggen, P.L., Morey, G.B., Hinze, W.J., Anderson, R.R., 1989. Interpretation of seismic reflection, gravity, and magnetic data across Middle Proterozoic Mid-Continent Rift system, Northwestern Wisconsin, Eastern Minnesota, and Central Iowa. Am. Assoc. Pet. Geol. Bull. 73 (3), 261–275.

Constable, S., 2006. SEO3: a new model of olivine electrical conductivity. Geophys. J. Int. 166 (1), 435–437. http://dx.doi.org/10.1111/j.1365-246X.2006.03041.x.

Dai, L., Karato, S.i., 2014. High and highly anisotropic electrical conductivity of the asthenosphere due to hydrogen diffusion in olivine. Earth Planet. Sci. Lett. 408, 79–86. http://dx.doi.org/10.1016/j.epsl.2014.10.003.

Dmitriev, V., Berdichevsky, M., 1979. The fundamental model of magnetotelluric sounding. Proc. IEEE 67 (7), 1034–1044. http://dx.doi.org/10.1109/PROC.1979.11386.

Doherty, L.H., 1963. Electrical conductivity of the Great Lakes. J. Res. Natl. Bur. Stand. D, Radio Sci. 67D (6), 765–771.

Ducea, M.N., Park, S.K., 2000. Enhanced mantle conductivity from sulfide minerals, Southern Sierra Nevada, California. Geophys. Res. Lett. 27 (16), 2405–2408. http://dx.doi.org/10.1029/2000GL011565.

Egbert, G.D., 1997. Robust multiple-station magnetotelluric data processing. Geophys. J. Int. 130 (2), 475–496.

Egbert, G.D., Booker, J.R., 1986. Robust estimation of geomagnetic transfer functions. Geophys. J. R. Astron. Soc. 87 (1), 173–194. http://dx.doi.org/10.1111/j.1365-246X.1986.tb04552.x.

Egbert, G.D., Kelbert, A., 2012. Computational recipes for electromagnetic inverse problems. Geophys. J. Int. 189, 251–267.

Hasterok, D., Chapman, D.S., 2011. Heat production and geotherms for the continental lithosphere. Earth Planet. Sci. Lett. 307, 59–70. http://dx.doi.org/10.1016/j.epsl.2011.04.034.

Heidlauf, D.T., Hsui, A.T., Klein, G.D., 1986. Tectonic subsidence analysis of the Illinois Basin. J. Geol. 94 (6), 779–794. http://www.jstor.org/stable/30071583.

Hildebrand, T., 1985. Magnetic terranes in the central United States determined from the interpretation of digital data. In: The Utility of Gravity and Anomaly Maps, pp. 248–266.

Hinze, W.J., Allen, D.J., Fox, A.J., Sunwood, D., Woelk, T., Green, A.G., 1992. Geophysical investigations and crustal structure of the North American Midcontinent Rift system. Tectonophysics 213, 17–32.

Hoffman, P.F., 1989. Precambrian geology and tectonic history of North America. In: The Geology of North America, pp. 447–512.

Holm, D., Anderson, R., Boerboom, T., Cannon, W., Chandler, V., Jirsa, M., Miller, J., Schneider, D., Schulz, K., Schmus, W.V., 2007. Reinterpretation of Paleoproterozoic accretionary boundaries of the north-central United States based on a new aeromagnetic–geologic compilation. Precambrian Res. 157, 71–79. http://dx.doi.org/10.1016/j.precamres.2007.02.023.

Jones, A.G., Lezaeta, P., Ferguson, I.J., Chave, A.D., Evans, R.L., Garcia, X., Spratt, J., 2003. The electrical structure of the Slave craton. Lithos 71, 505–527. http://dx.doi.org/10.1016/j.lithos.2003.08.001.

Jones, A.G., Ledo, J., Ferguson, I.J., 2005. Electromagnetic images of the Trans-Hudson orogen: the North American Central Plains anomaly revealed. Can. J. Earth Sci. 42 (4), 457–478. http://dx.doi.org/10.1139/e05-018.

Jones, A.G., Fullea, J., Evans, R.L., Muller, M.R., 2012. Water in cratonic lithosphere: calibrating laboratory-determined models of electrical conductivity of mantle minerals using geophysical and petrological observations. Geochem. Geophys. Geosyst. 13 (6), Q06010. http://dx.doi.org/10.1029/2012GC004055.

Kelbert, A., Meqbel, N., Egbert, G.D., Tandon, K., 2014. ModEM: a modular system for inversion of electromagnetic geophysical data. Comput. Geosci. 66, 50–53.

Keller, G.R., 2013. The Moho of North America: a brief review focused on recent studies. Tectonophysics 609 (0), 45–55. http://dx.doi.org/10.1016/j.tecto.2013.07.031.

Keller, G.R., Lidiak, E.G., Hinze, W.J., Braile, L.W., 1983. The role of rifting in the tectonic development of the midcontinent, USA. Tectonophysics 94 (1–4), 391–412. http://dx.doi.org/10.1016/0040-1951(83)90026-4.

McKenzie, D., Jackson, J., Priestley, K., 2005. Thermal structure of oceanic and continental lithosphere. Earth Planet. Sci. Lett. 233, 337–349. http://dx.doi.org/10.1016/j.epsl.2005.02.005.

Meqbel, N.M., Egbert, G.D., Wannamaker, P.E., Kelbert, A., Schultz, A., 2014. Deep electrical resistivity structure of the northwestern U.S. derived from 3-D inversion of USArray magnetotelluric data. Earth Planet. Sci. Lett. 402, 290–304. http://dx.doi.org/10.1016/j.epsl.2013.12.026.

Merino, M., Keller, G.R., Stein, S., Stein, C., 2013. Variations in Mid-Continent Rift magma volumes consistent with microplate evolution. Geophys. Res. Lett. 40 (8), 1513–1516. http://dx.doi.org/10.1002/grl.50295.

Newell, K.D., Hatch, J.R., 2000. A petroleum system for the Salina Basin in Kansas based on organic geochemistry and geologic analog. Nat. Resour. Res. 9 (3), 169–200. http://dx.doi.org/10.1023/A:1010151614263.

Nicholson, S.W., Schulz, K.J., Shirey, S.B., Green, J.C., 1997. Rift-wide correlation of 1.1 Ga Midcontinent rift system basalts: implications for multiple mantle sources during rift development. Can. J. Earth Sci. 34 (4), 504–520. http://dx.doi.org/10.1139/e17-041.

Nieuwenhuis, G., Unsworth, M.J., Pana, D., Craven, J., Bertrand, E., 2014. Three-dimensional resistivity structure of Southern Alberta, Canada: implications for Precambrian tectonics. Geophys. J. Int. 197 (2), 838–859. http://dx.doi.org/10.1093/gji/ggu068.

Ogawa, Y., Jones, A.G., Unsworth, M.J., Booker, J.R., Lu, X., Craven, J., Roberts, B., Parmelee, J., Farquharson, C., 1996. Deep electrical conductivity structures of the Appalachian Orogen in the southeastern U.S. Geophys. Res. Lett. 23 (13), 1597–1600. http://dx.doi.org/10.1029/95GL03601.

Patro, P.K., Egbert, G.D., 2008. Regional conductivity structure of Cascadia: preliminary results from 3D inversion of USArray transportable array magnetotelluric data. Geophys. Res. Lett. 35 (20), L20311. http://dx.doi.org/10.1029/2008GL035326.

Renee Rohs, C., Van Schmus, W., 2007. Isotopic connections between basement rocks exposed in the St. Francois Mountains and the Arbuckle Mountains, southern mid-continent, North America. Int. J. Earth Sci. 96 (4), 599–611. http://dx.doi.org/10.1007/s00531-006-0123-5.

Schulz, K.J., Cannon, W.F., 2007. The Penokean orogeny in the Lake Superior region. Precambrian Res. 157 (1–2), 4–25. http://dx.doi.org/10.1016/j.precamres.2007.02.022.

Shen, W., Ritzwoller, M.H., Schulte-Pelkum, V., 2013. Crustal and uppermost mantle structure in the central U.S. encompassing the Midcontinent Rift. J. Geophys. Res., Solid Earth 118 (8), 4325–4344. http://dx.doi.org/10.1002/jgrb.50321.

Sleep, N.H., Sloss, L.L., 1978. A deep borehole in the Michigan Basin. J. Geophys. Res., Solid Earth 83 (B12), 5815–5819. http://dx.doi.org/10.1029/JB083iB12p05815.

Southwick, D.L., Morey, G.B., 1990. Tectonic imbrication and foredeep development in the Penokean Orogen, east-central Minnesota — an interpretation based on regional geophysics and the results of test-drilling. U.S. Geol. Surv. Bull. 1903-C, C1–C17.

Stein, C.A., Stein, S., Merino, M., Randy Keller, G., Flesch, L.M., Jurdy, D.M., 2014. Was the Midcontinent Rift part of a successful seafloor-spreading episode? Geophys. Res. Lett. 41 (5), 1465–1470. http://dx.doi.org/10.1002/2013GL059176.

Sternberg, B.K., Clay, C.S., 1977. The Earth's Crust: Its Nature and Physical Properties. American Geophysical Union, pp. 501–530.

Van Schmus, W., Schneider, D., Holm, D., Dodson, S., Nelson, B., 2007. New insights into the southern margin of the Archean–Proterozoic boundary in the north-central United States based on U–Pb, Sm–Nd, and Ar–Ar geochronology. Precambrian Res. 157 (1), 80–105.

Wang, D., Karato, S.i., Jiang, Z., 2013. An experimental study of the influence of graphite on the electrical conductivity of olivine aggregates. Geophys. Res. Lett. 40 (10), 2028–2032. http://dx.doi.org/10.1002/grl.50471.

Wannamaker, P.E., 2005. Anisotropy versus heterogeneity in continental solid earth electromagnetic studies: fundamental response characteristics and implications for physicochemical state. Surv. Geophys. 26 (6), 733–765. http://dx.doi.org/10.1007/s10712-005-1832-1.

Wannamaker, P.E., Doerner, W.M., Stodt, J.A., Johnston, J.M., 1997. Subdued state of tectonism of the Great Basin interior relative to its eastern margin based on deep resistivity structure. Earth Planet. Sci. Lett. 150, 41–53. http://dx.doi.org/10.1016/S0012-821X(97)00076-9.

Wunderman, R.L., 1988. Crustal structure across the exposed axis of the Midcontinent Rift and adjacent flanks, based on magnetotelluric data, Central Minnesota–Wisconsin: a case for crustal inhomogeneity and possible reactivation tectonics. Ph.D. thesis. Michigan Technological University.

Yoshino, T., Noritake, F., 2011. Unstable graphite films on grain boundaries in crustal rocks. Earth Planet. Sci. Lett. 306 (3–4), 186–192. http://dx.doi.org/10.1016/j.epsl.2011.04.003.

Yuan, H., Romanowicz, B., 2010. Lithospheric layering in the North American craton. Nature 466 (7310), 1063–1068. http://dx.doi.org/10.1038/nature09332.

Yuan, H., French, S., Cupillard, P., Romanowicz, B., 2014. Lithospheric expression of geological units in central and eastern North America from full waveform tomography. Earth Planet. Sci. Lett. 402, 176–186. http://dx.doi.org/10.1016/j.epsl.2013.11.057.

Zhdanov, M.S., Smith, R.B., Gribenko, A., Cuma, M., Green, M., 2011. Three-dimensional inversion of large-scale EarthScope magnetotelluric data based on the integral equation method: geoelectrical imaging of the Yellowstone conductive mantle plume. Geophys. Res. Lett. 38 (8), L08307. http://dx.doi.org/10.1029/2011GL046953.